

A Comparative Study on the Production of a Hat Profile by Roll Forming and Stamping

Timon Suckow,* Ezgi Bütev Öcal, and Peter Groche

Lightweight design using high-strength aluminum alloys has gained importance due to the continuing need for weight reduction and increasing crash safety requirements in the automotive industry. There are various manufacturing processes available for processing high-strength aluminum alloys. Herein, the production of high-strength aluminum parts by roll forming and stamping based on the example of an AA7075-T6 hat profile is compared. Roll forming represents a continuous manufacturing process, while stamping is a discontinuous process. Different process routes (T6, W-Temper and O) for roll forming as well as for stamping (T6, W-Temper, O and hot forming) are in focus of the investigation. Fundamental differences of the forming processes and the tempering condition are observed and criteria for the choice of the manufacturing process and process route are presented. The temperature-supported process routes improve the poor cold formability of AA7075 alloy and thus enhance the process window. Potential is offered for both manufacturing processes by applying tailored properties achieved through targeted quenching.

1. Introduction

The high-strength aluminum alloy AA7075 is presently applied in high-tech industries such as aerospace, high-end sports equipment, or bicycles. Due to increasing lightweight demands in the automotive industry, an expansion is conceivable. With regard to the automotive industry, the use of mass production processes is reasonable due to high production volumes. Poor formability is one of the disadvantages of the AA7075 alloy. However, temperature-supported processes lead to an improvement in formability. These include hot forming (HF),^[1] warm forming,^[2] W-Temper forming,^[3] and forming in the soft annealed state (O) of the material.^[4] In current applications, the alloy AA7075 is mainly used in the high-strength T6-state or in an overaged state (e.g., T73). An exception is given by the targeted application

of tailored mechanical properties, thanks to the high quenching sensitivity of the AA7075 alloy. Different quenching rates after solution annealing (SA) lead to different mechanical properties.^[5,6]

HF of AA7075 in the context of this study is HF and die quenching with cold or heated tools. During HF, the forming temperature is reported to be in the range of the SA temperature of the AA7075 alloy.^[1,7] Within this process route, the forming occurs during quenching in the forming tool.^[1] After forming, artificial aging is required to achieve the T6-state.

During warm forming, the temperature is in the range of $T = 140\text{--}230\text{ }^{\circ}\text{C}$.^[2,8] Formability is increased thanks to the high forming temperature. Depending on the initial material state, the forming temperature, and the holding time, post heat treatment may be required to achieve the

T6-state after forming.

Forming in the W-Temper- or O-state provides another option for temperature-supported process routes. Both process routes have in common that the forming takes place in a cold state. This is advantageous in terms of cycle times, lower complexity of process control, less investment, less wear and galling, and simple tool design.^[3,7] The W-Temper-state is obtained after SA and quenching and increases formability for a limited time after quenching. After forming and artificial aging, the T6-condition is achieved again. The O-process route is characterized by forming the material in the O-state. The soft annealed state is achieved by heat treatment of at least 9 h in the temperature range of $T = 230\text{--}410\text{ }^{\circ}\text{C}$.^[9] During this process route, post heat treatment is time-consuming, as the material requires SA, quenching, and artificial aging in order to achieve the T6-state.

Recent examples of cold forming in the high-strength T6-state are given by other studies,^[10,11] both in roll forming. An advantage is that no heat treatment is necessary. Disadvantages are the low formability, which leads to cracks already at moderate strain levels and the high springback after forming.

Figure 1a shows the different process routes with regard to the forming temperature and the integration of the forming process into the process chain. During forming in the T6-state, no heat treatment is necessary for the whole process chain. The other process routes require heat treatments before, during, or after forming to increase formability and obtain the desired mechanical properties. The stress-strain diagrams for the different material states during forming show the increase in formability (Figure 1b). The curve at $T = 400\text{ }^{\circ}\text{C}$ is characteristic for the HF process.

T. Suckow, E. Bütev Öcal, P. Groche
Institute for Production Engineering and Forming Machines
Technical University of Darmstadt
Otto-Berndt-Str. 2, 64287 Darmstadt, Germany
E-mail: timon.suckow@ptu.tu-darmstadt.de

The ORCID identification number(s) for the author(s) of this article can be found under <https://doi.org/10.1002/adem.202201877>.

© 2023 The Authors. Advanced Engineering Materials published by Wiley-VCH GmbH. This is an open access article under the terms of the Creative Commons Attribution-NonCommercial License, which permits use, distribution and reproduction in any medium, provided the original work is properly cited and is not used for commercial purposes.

DOI: 10.1002/adem.202201877

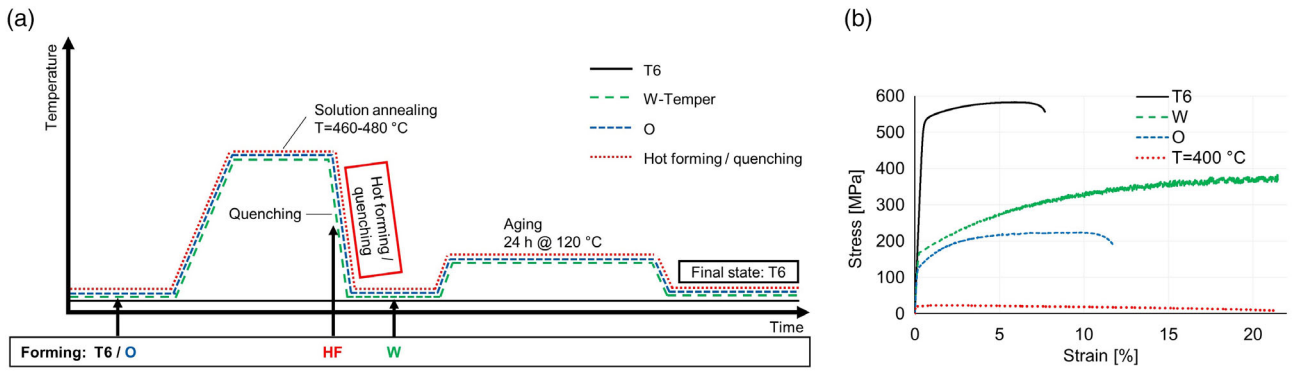


Figure 1. a) Process routes for forming the high-strength aluminum alloy AA7075. b) Stress–strain diagrams for the AA7075 alloy in different conditions.

As there is no such comparison between continuous and discontinuous manufacturing processes so far; the present study aims to give a detailed overview. The production of a hat profile serves as an example. Contents of the comparative study are the process design in terms of tool design, design of the heat treatment, and FE analysis. Furthermore, product quality is assessed regarding formability, geometrical accuracy, forming forces, and surface quality. Potential and challenges for the application of tailored properties by targeted quenching are investigated for roll forming as well as for stamping. Finally, the differences, advantages, disadvantages, and challenges of the respective processes and process routes are identified and discussed to provide an overview as well as a recommendation for the choice of the process.

2. Process Design

Process design is of high importance for achieving the desired final properties in processing the AA7075 alloy since the process windows for forming and heat treatment are small. The process design includes temperature control before, during, and after forming, as well as forming parameters (e.g., tool geometry, bending radii, step sequence). The procedure for process design presented in this study is summarized in **Figure 2**.

The process design starts with defining the target geometry and the desired material properties. The core of the process design is the tool design, the design of the heat treatment, and the FE analysis. Tool design is mostly based on empirical

values and the experience of the designer. For advanced applications, the tool design is also based on an FE analysis. The FE analysis is conducted simultaneously with the tool design and design of the heat treatment. The target geometry is evaluated from the FE model, while the desired material properties have to be determined from pre-experiments that simulate the heat treatment cycles of the entire process chain as accurately as possible. After meeting the targets, the design of the manufacturing process in terms of the industrial application is as follows. The last step is the production of the hat profile.

2.1. Process Chains

Within this study, several process routes for the manufacturing processes roll forming and stamping are investigated. Roll forming is a bending process with rotating tool movement for the production of open and closed profiles and usually takes place at room temperature.^[12] During roll forming, the sheet is formed in several forming passes, each consisting of top, bottom, and sometimes side rolls. The shape of the roll gap forms the sheet material into the desired shape.

Thanks to the continuous material flow, roll forming offers a high potential for integrating further processes before, during, or after roll forming.^[12] Part of the heat treatments can be performed inline.^[13] On the other side, stamping is a discontinuous forming process. During stamping, the sheet is placed in a tool consisting of a die and a punch and then formed. **Figure 3** and **4** show the process routes for roll forming and stamping of the

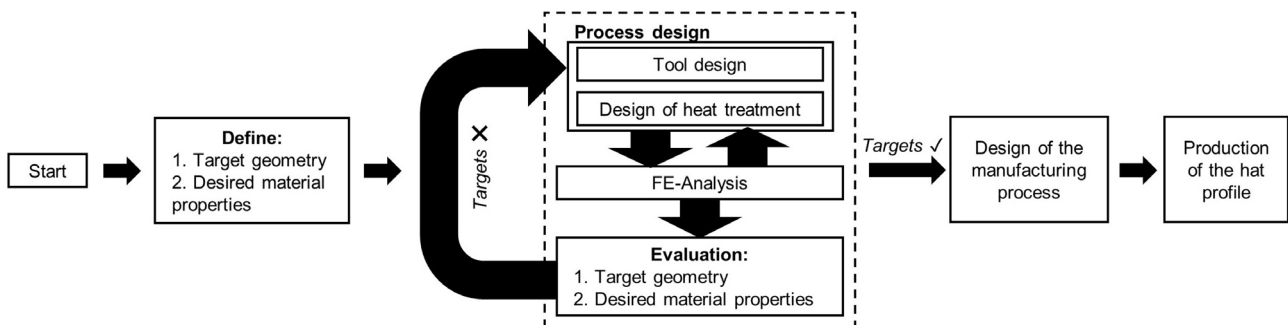


Figure 2. Process design procedure for the development of a temperature-supported forming process.

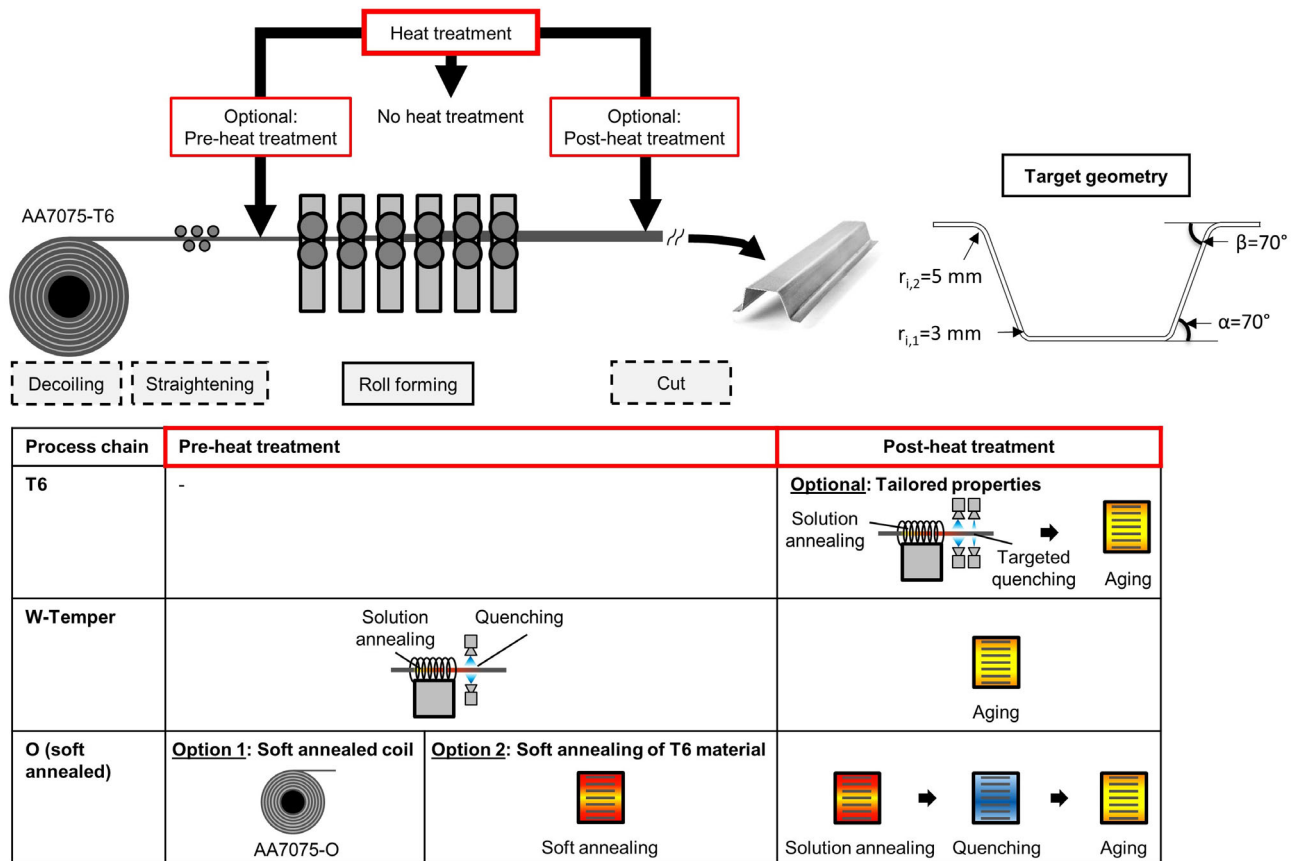


Figure 3. Process routes for roll forming of an AA7075 hat profile.

hat profile including pre-, in-process-, and postheat treatment, respectively. The profile can be manufactured in various process routes starting from a coil in the peak aged T6-state. Cold forming in the high-strength T6-state on the one hand and temperature-supported HF-, W-Temper-, and O-process routes on the other.

For roll forming, one advantage of the W-Temper process is integrating the preheat treatment by induction heating and water spray quenching inline before forming. On the contrary, an inline W-temper heat treatment is not possible for stamping because of the discontinuous forming process. Therefore, a separate furnace is used for the W-temper process and the heat-treated samples need to be transferred to the forming tool. For the heat treatment of the process route in the O-state, there is the option of using a soft annealed coil or soft annealing sheets for both processes. The disadvantage is the high-energy requirement for soft annealing, as the heat treatment cycle is long and the temperature is high.^[9]

After forming, postheat treatment allows the adjustment of the material properties. The target condition is the peak aged T6-state. After the W-Temper process chain, the material is peak aged for 24 h at 120 °C. After the O-process route of roll forming, SA, quenching, and artificial aging, 24 h, 120 °C, are required.

Furthermore, tailored properties can be achieved by targeted quenching for roll forming and stamping in the postheat treatment. For example, by targeted water quenching with a sharp spatial transition to air cooling after the forming process, this approach is suitable for roll forming and stamping. Additionally,

stamping allows the application of tailored properties by targeted quenching in a separated hot/cold tool.^[6]

The geometry of the hat profile for roll forming and stamping is shown in Figure 3 and 4, respectively. The initial sheet thickness is $s = 1.5$ mm for both processes. For roll forming the initial sheet width is $s = 170$ mm and for stamping $s = 200$ mm. While roll forming allows the production of any desired length, limited to the length of the coil, the length of the stamped part is limited to the length of the assembly space of the press and the size of the forming tool. The length of the stamped part is $l = 260$ mm within this study. Prior to tool design, the technical requirements for the parts to be produced are defined in terms of the target geometry and material properties. In terms of geometry, a low deviation from the desired geometry is advantageous, as the springback compensation leads to high effort during process design. Another objective is to achieve a high level of strength equivalent to the strength of the alloy in the high-strength T6 state. A good surface quality is also aimed for. This means a sheet surface without function-limiting scratches and ideally without visible scratches.

2.2. Tool Design

2.2.1. Roll Forming

Tool design in roll forming is supported by application-specific software packages such as Ubeco PROFIL^[14] or COPRA RF.^[15]

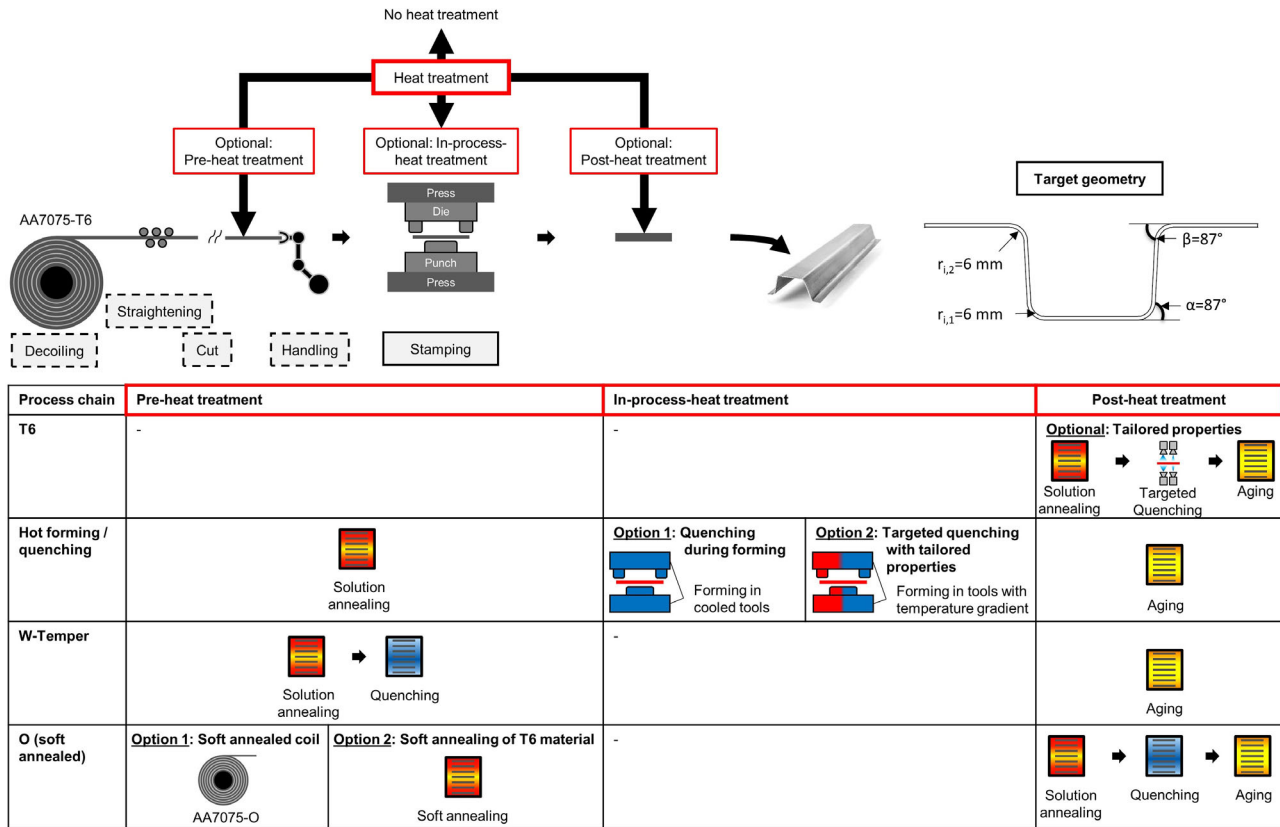


Figure 4. Process routes for stamping of an AA7075 hat profile.

The geometry of the forming rolls is generated in these software packages and transferred to FE solver. Parameters in tool design to be varied are, on the one hand, the selection of the tool material and, on the other hand, the profile flower, bending angles, bending radii, and roll diameters and interstation distance.^[12] Tool design is not too complex since roll forming is a cold forming process in general. However, the experience of the roll designer is important in order to avoid typical defects during roll forming and achieve high efficiency by not using too many passes.^[12] After successful process design and meeting the defined targets in terms of profile geometry and properties of the final part, the tool is ready for manufacturing.

2.2.2. Stamping

Tool design is performed in the CAD Software (e.g., AutoCAD, NX, and SolidWorks) according to the needs for the process design. The geometry of the die and the punch are defined based on the target drawing depth. Similar to roll forming, FE analysis of the forming process is conducted during process design.

In tool design, stamping in the hot and cold conditions of the sheet and the tools is taken into account. Therefore, the blank holders, punches, and dies are designed for placing suitable heating units and cooling pipes inside of them. In addition, insulation is added just below the heated section in order to protect it from heat. Thermal expansion is also considered for the process design of the HF-quenching process because it is expected to

have height differences between heated and cooled sections after heating to elevated temperatures.

2.2.3. Heat Treatment

With regard to process design, heat treatments are of interest in both forming processes. Small deviations from the heat treatment cycle lead to deviations in the material properties and thus to undesired deviations in the final product. These include divergences from the target SA temperature of 460–480 °C and uneven temperature distribution during SA.^[13] Furthermore long transfer times of the hot sheet to the quenching unit and thus an unintended temperature drop before quenching or uneven quenching cause undesired mechanical properties. Therefore, process design of the heat treatment is of great importance. Design parameters include the choice of the heating method (e.g., furnace or induction) and the transfer between heating and quenching.

2.3. FE Analysis

In the beginning of the process design, an FE model for each manufacturing process is developed. The aim of the numerical simulation is to predict process parameters and the target geometry with low effort and thus save time, effort, and money.^[16] Once the targets are achieved, the FE model is the basis for tool design.

2.3.1. Roll Forming

The final geometry of the hat profile as well as the forming section are presented in **Figure 5a**. The forming section is previously given and consists of six forming passes. After six forming passes, the final geometry is produced. The higher bending angle α in pass 5, compared with pass 6, is for springback compensation. The FE model is set up according to the principle: as simple as possible and as detailed as necessary, which maximizes efficiency during process design. Friction is neglected since the effect on the results regarding the final geometry of the part is small.^[17]

Further boundary conditions and the setup of the FE model are shown in **Figure 5b**. Independent of the process route, purely mechanical simulation models are sufficient for roll forming since the forming itself takes place in the cold state. Thus, the effort to determine the flow curves by uniaxial tensile tests is low, as they are generated on a standard testing machine in the cold state (T6, W-Temper, and O).

2.3.2. Stamping

The FE model for the stamping process depends on the process route. A 2Dl model is sufficient for the process routes T6, W-Temper, O, and HF, as neglectable through sheet-length effects occur. For targeted quenching, in order to apply tailored mechanical properties in the length direction of the part, a 3D FE model is required. **Figure 6** shows the FE models for the stamping process. Due to the geometrical symmetry of the stamping tool and the blank, only half of the experimental setup was implemented in the FE model.

The tools are modeled rigid and the mechanical contact interaction properties are classified into normal and tangential behavior, referring to the friction between the two contact surfaces. In the FE simulation, the penalty contact method is used because the contact pair contains a rigid surface, allowing an elastic slip of the surfaces when they should be sticking. The frictional coefficient is dependent on the sheet temperature. Similar to the FE model for the roll forming process, the flow curves for the T6-,

W-Temper-, and O-process routes are obtained by uniaxial tensile tests on a standard testing machine. Higher effort is required to obtain the flow curves for the HF process routes, as shown in ref. [1].

3. Experimental Section

All experiments within this study were conducted with the high-strength aluminum alloy AA7075. Initially, the alloy was in the T6-state. **Table 1** shows the chemical composition of the alloy.

3.1. Roll Forming

The roll forming experiments for each process route were performed on a VOEST P450/4 roll forming machine. No lubricant was used in the experiments. The distance between two passes was 520 mm, the sheet velocity was 1 m min^{-1} , and the sheet length was 2000 mm. To minimize the slip, the roll gap of 1.2 was 0.3 mm smaller than the sheet thickness. The hardened cold work tool steel 1.2379 (X155CrVMo12-1) was used for the rolls. **Figure 7a** shows the experimental setup for the roll forming experiments.

Temperature-supported process routes in roll forming require additional heat treatment before and after forming. As illustrated in **Figure 1** and **3**, different process routes require customized heat treatments to achieve desired final properties. Thanks to the continuous material flow during roll forming, it is possible to integrate short-time heat treatment inline. Examples of short-time heat treatments are the SA as preheat treatment before forming in the W-Temper-process route and the postheat treatment after forming with the aim to achieve tailored properties. Both were integrated into the process chain by induction heating and water quenching.

Figure 7b shows the experimental setup for the W-Temper inline heat treatment. The quality of the heat treatment and material properties after the forming process are shown in ref. [13]. For the inline heat treatment during roll forming, additional parameters were the application of strip tension to reduce

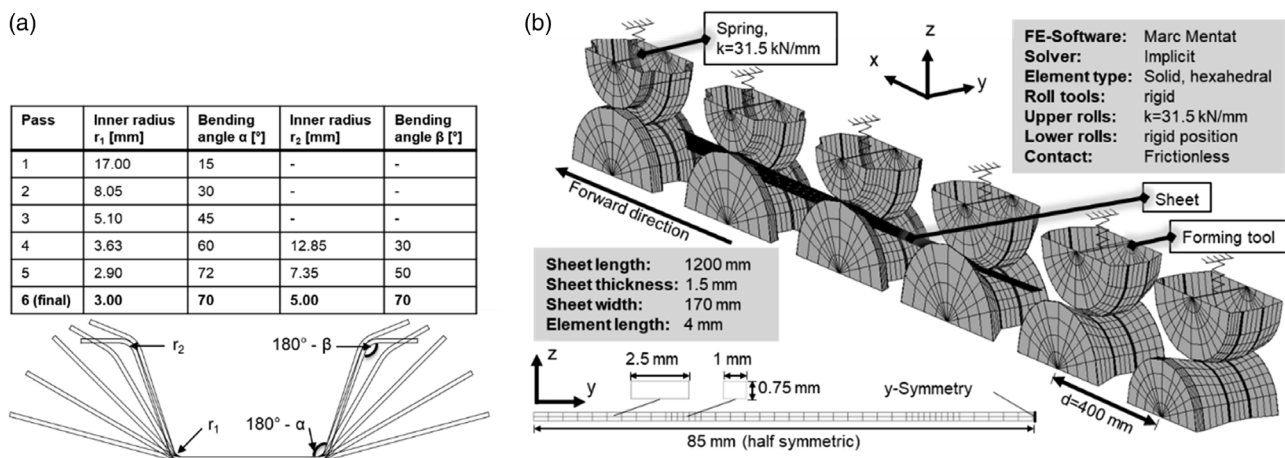


Figure 5. Forming section a) and FE model b) for the roll forming process.

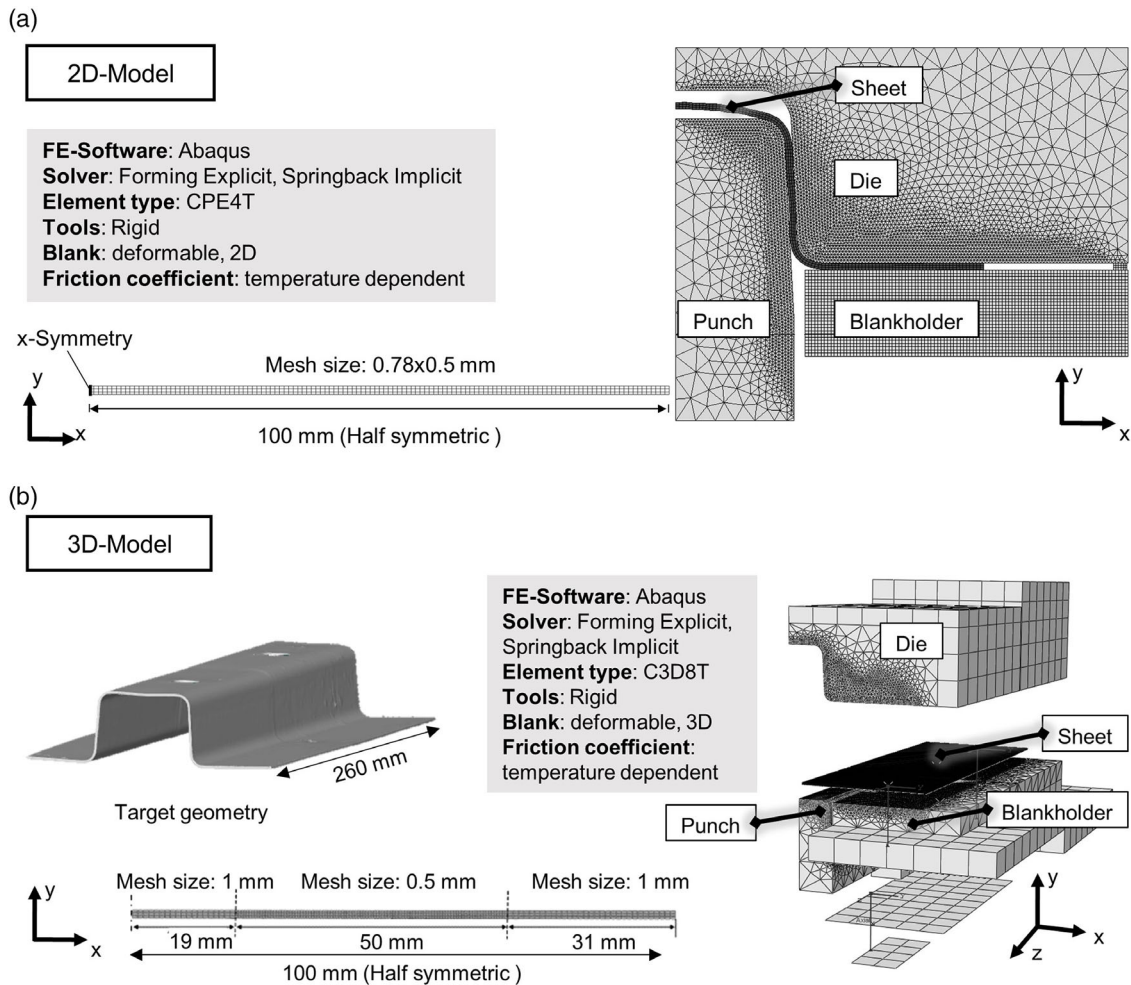


Figure 6. a) 2D and b) 3D FE model for the stamping process.

Table 1. Chemical composition of the AA7075 alloy.

Element	Si	Fe	Cu	Mn	Mg	Cr	Zn	Ti	Zr
Weight [%]	0.08	0.12	1.6	0.04	2.7	0.19	5.9	0.05	0.04

unwanted distortion before roll forming, the choice of quenching method (e.g., water-spray, mixed water- and air-spray or water bath), and the process speed. During the quenching process, controllable spray nozzles were used for applying different cooling rates on the sheet.

3.2. Stamping

The stamping experiments were conducted in a servo motor press (**Figure 8**). The tool for the stamping experiments was placed into a Synchronpress (SWP2500) having a maximum force of 250 kN and a maximum speed of 180 mm s^{-1} . The tool consisted of the blank holders and punches at the bottom part and the die at the upper part. The drawing depth was set to 40 mm for this process. Since the tool was designed for cold

and HF processes, the hardened hot-working steel Uddeholm Unimax (57 HRC) was used as tool material. The rest of the parts, including the upper and lower parts, were made of C45 steel. For the cold forming process routes (T6, W-Temper, and O), the oil-based lubricant, Putrol NWV 1933-30N-1, was used in order to decrease the effect of wear and friction during forming. During the HF process, a heat resistant boron nitride/water suspension was used.

Unlike roll forming, in stamping, inline heat treatment is not possible because of the discontinuous forming process. The manufactured tool was placed on the press and heat treatment furnace was located in a separate place. AA7075 alloy sheets were solution annealed at 480°C for 15 min and then transferred as quickly as possible to the forming tool. SA was conducted in a Nabertherm NA 15/65 convection furnace.

A variation of the HF and quenching process was the production of functionally tailored products from high-strength aluminum AA7075-T6 alloy, aiming at a high degree of shape accuracy. For this purpose, the local modification of the tailored properties in the hat profile was obtained through the use of different cooling conditions during the quenching process inside the tools. The left part of the die was actively heated while the right part

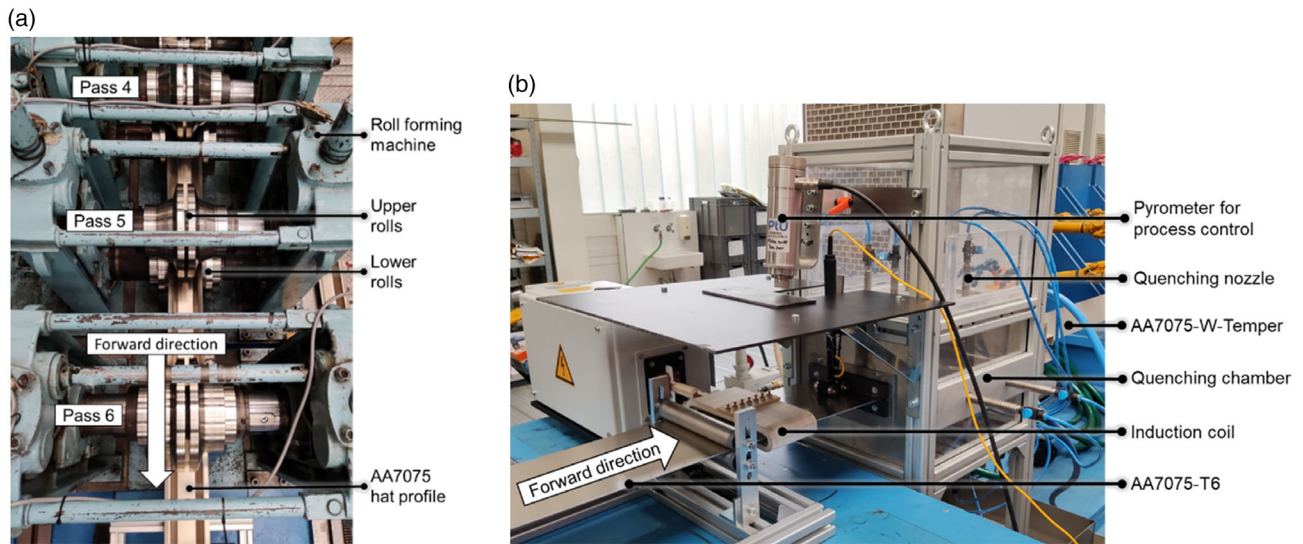


Figure 7. a) Experimental setup for the roll forming experiments and b) for the inline heat treatment.

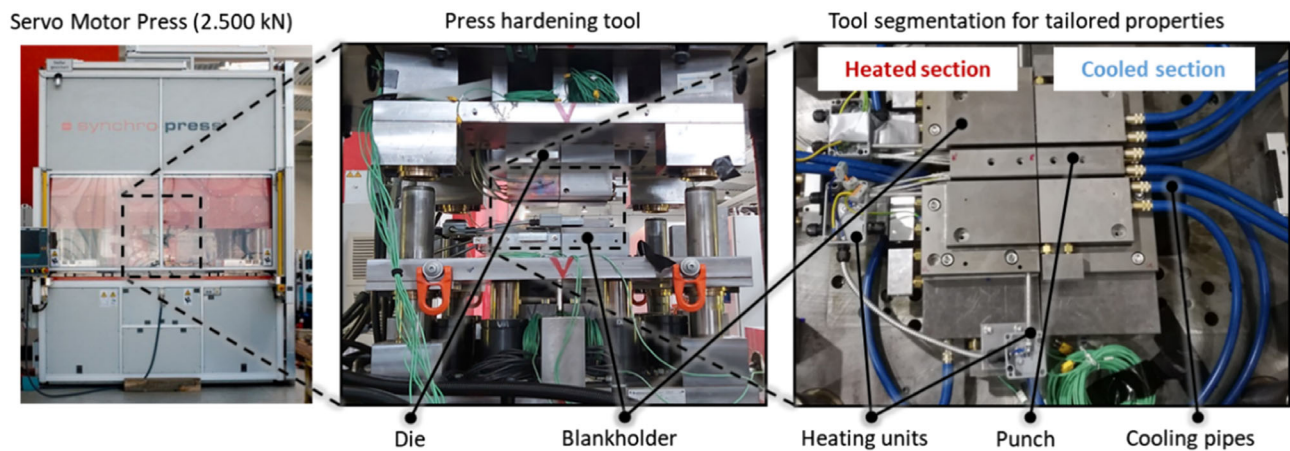


Figure 8. Experimental setup for the stamping process.

was cooled with flowing water depicted by blue cooling pipes, as shown in Figure 8. The temperature of the cooled die was kept constant around room temperature; at the same time, the temperature of the heated side was maintained at $T = 300\text{ °C}$ by heating cartridges in the punch and the die and tubular heaters in the blank holder. The quenching and forming process took place simultaneously in the tool. Afterward, the hat-shaped profiles were cooled down in water and subsequently artificially aged at 120 °C for 24 h.

3.3. Discontinuous Heat Treatments for Thermomechanical Processing

Most of the investigated process routes required heat treatments to increase the formability of the material. **Table 2** shows the devices and boundary conditions for discontinuous heating for the pre- and postheat treatments. Discontinuous heat treatments, which required a furnace for heating, were SA, artificial aging, and soft annealing.

Table 2. Discontinuous heat treatments for several process routes, using a furnace.

Heat treatment	SA	Artificial aging	Soft annealing	
Process	Stamping	Roll forming and Stamping	Roll forming	Stamping
Furnace	Nabertherm NA 15/65	Binder FDL 115	External	Nabertherm NA 15/65
Temperature	15 min at 480 °C	24 h at 120 °C	2 h at 410 °C , Ramp $410\text{--}230\text{ °C}$ (6 h), 2 h at 230 °C	

3.4. Measurement Methods

3.4.1. Tensile Tests

In the present study, the tensile tests were conducted using a Zwick Roell 100 kN universal testing machine with a video extensometer (videoXtens) for strain measurement. The tensile specimen geometry for roll forming was in accordance with DIN 50 125.^[18] On the contrary, subsized flat tensile test samples cut from the top surface of the hat-shaped profile were used for stamping, according to the study of Kumar et al.^[19] As a result of the tensile tests, the characteristic values for the evaluation of the mechanical properties were obtained from the resulting stress–strain diagram.

3.4.2. Hardness Measurement

Hardness measurement was conducted with samples cut from the cross section of the formed parts and subsequently embedded in epoxy resin and polished. A Struers DuraScan 20 hardness testing machine was utilized to measure the Vickers hardness.

3.4.3. Geometry Measurement

For the experimentally produced parts, geometry measurement was conducted with the GOM ATOS 5 3D scanning system. From the measured point cloud, cross sections, profile deformations, etc. were extracted.

3.4.4. Forming Force

For roll forming, load cells of type HBM C9B were attached to the forming passes, according to the experimental setup in ref. [17]. During stamping, the force of the SynchroPress was measured by two parallel load cells.

3.4.5. 3D Surface Examination

In order to investigate the surface quality of the produced parts, a 3D surface examination was conducted. For examination, a section (20 × 20 mm) of the produced part was cut and investigated optically with a confocal μ Surf microscope from Nanofocus (Confocal Microscope μ Surf).

4. Results and Discussion

4.1. Process and Part Quality

4.1.1. Formability

In the beginning of this section, it is mentioned that the target geometries in both processes are slightly different. The main difference lies in the bending radius, which is smaller for the roll forming process. Formability of the high-strength aluminum alloy is limited in the high-strength T6-state. Therefore, the alloy is mainly formed in temperature-supported process routes. In this section, different process routes are shown with regard to formability. During roll forming in the high-strength T6-state,

material failure occurs in the third pass in the form of cracks. The inner bending radius is $r_1 = 5.10$ mm and the bending angle is $\alpha = 45^\circ$ when failure occurs. No failure occurs during stamping for all process routes. An advantage of the stamping process is the use of distancing between the blank holder and the die, leading to a change in the contact force. The smaller distancing height increases the contact area and the contact pressure, resulting in fracture. Using distancing, the die has no direct contact with the blank holder. In the present study, a constant distancing of 1.5 mm is used.

For a general statement, the profile geometries need to be identical. However, in roll forming the forming strategy and in stamping the fine adjustment of the tool are important with regard to the process limits, which make it even more difficult to draw a general statement.

4.1.2. Geometrical Accuracy

In the context of process and component quality, geometric accuracy is of great importance. Deviations from the nominal geometry are acceptable up to geometry-dependent limits according to DIN EN 10 162, where a maximum deviation of the bending angle of $\alpha \pm 1,15^\circ$ is acceptable.^[20] The investigation is focused on geometrical errors in the cross section, represented by the bending angle. **Figure 9** shows the cross section of the profiles after forming and springback. The springback angle α_s is defined as the deviation between the target angle α and the bending angle after springback α_b .

Springback after roll forming is very small after the W-Temper- and O-process routes ($\alpha_s < 0.2^\circ$). One reason for the small springback is the compensation of the springback by overbending the bending angle α in stage 5. The other reason is the low yield strength of the material in the W-Temper- and O-state. For stamping, the difference between T6 and the temperature-supported processes is significant. While the springback angle $\alpha_s = 26^\circ$ is very high for the T6-process route, it can be reduced to $\alpha_s = 2.4^\circ$ for the HF process route. The difference between quenching in a cold ($T = 20^\circ\text{C}$) and hot ($T = 300^\circ\text{C}$) tool is small. Even for stamping, there is a high potential for temperature-supported cold forming process routes (W-Temper and O). For the W-Temper process route the springback angle is $\alpha_s = 7^\circ$ and for the O-process route $\alpha_s = 6^\circ$. However, springback is higher than with roll forming. For all stamping process routes, the springback angle is higher than the maximum allowed deviation of the bending angle, according to DIN EN 10 162.^[20] For interpretation of the results, it must be considered that the bending radius is larger with stamping than with roll forming, which leads to higher springback. In addition, compensation of the springback angle is also possible for stamping by overbending but it is not in the scope of this study.

4.1.3. Forming Force

The requirements for the machine and tools can be determined from the reaction forces during forming. **Figure 10a** shows the maximum forming force for roll forming and **Figure 10b** for stamping. In the first pass, the forming force in the T6-state is significantly higher than for the temperature-supported

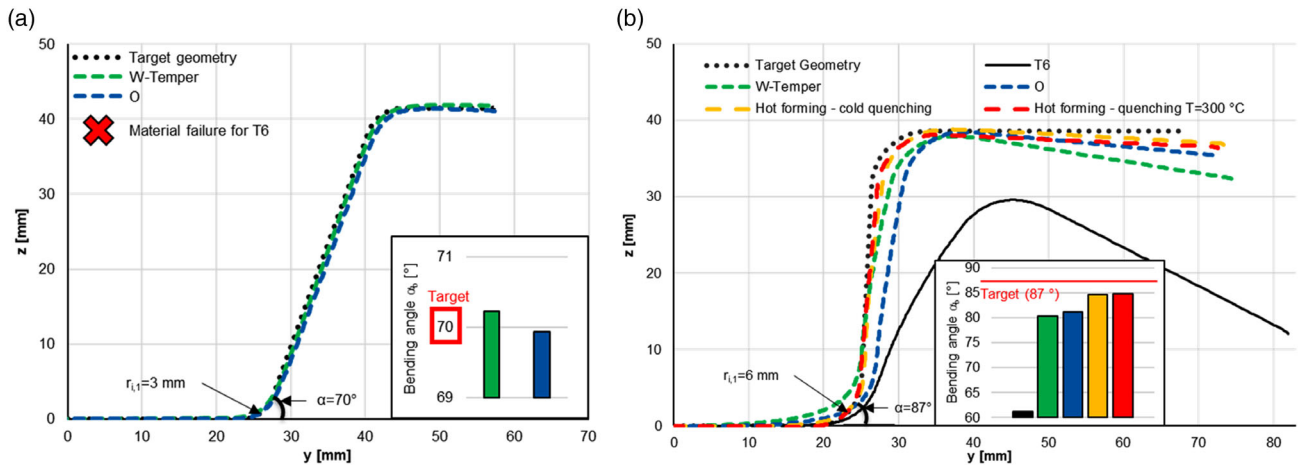


Figure 9. Cross section of the formed parts after a) roll forming and b) stamping.

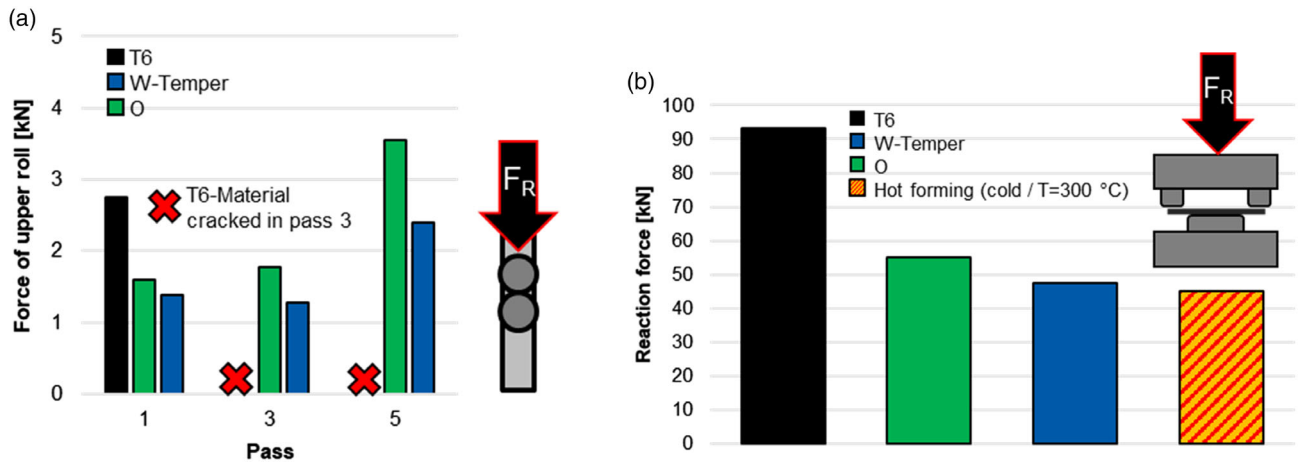


Figure 10. a) Force of the upper roll during roll forming. b) Forming force during stamping.

process routes. The maximum forming force during roll forming occurs in the fifth pass. Since the material cracks in the third pass, no results were obtained. As expected, the forces are lowest in the soft annealed material.

The highest reaction force in stamping is observed for T6-state, as expected. Similar to roll forming process, lower reaction forces are obtained in the temperature-supported process routes. In addition to roll forming, the HF process route is investigated. The tool is divided into two sections: one with a temperature of $T = 20\text{ }^{\circ}\text{C}$ and one with a temperature of $T = 300\text{ }^{\circ}\text{C}$, in order to apply tailored mechanical properties on the formed sheet. Compared to roll forming, the forming force during stamping is much higher, which results in high requirements for the forming tool and the press. However, the force during stamping strongly depends on the length of the hat profile, while the length of the profile has no influence on the forming force during roll forming.

4.1.4. Surface Quality

An inadequate tribological system leads to tool wear, which in turn results in higher wear of the produced parts and thus a lower

surface quality during roll forming.^[21] According to another study,^[12] aluminum has to be carefully formed to avoid scratches during roll forming. This means a careful design of the tools, more passes, appropriate tool material, or tailored roll surface finish. Most important is the tribological system, mainly defined by the lubricant. This is also valid for the stamping process.^[22] In this section, the surface quality of the cold-formed parts, manufactured in temperature-supported process chains, is analyzed. For roll forming, the high contact normal stress in the inner side of the bending radii leaves a pressure zone that resembles a surface smoothing. This is shown in **Figure 11a** (locations 2 and 4). Wear in the form of scratches, however, occurs next to the outer bending radii (locations 1 and 3). This results from the relative velocity between the roll tools and the sheet metal and is intensified by the absence of lubricant in the experiments.^[12] The scratches are localized in a small area in the cross section of the profile.

For the stamped parts, wear in the form of scratches is observed at the wall surface that slides over the radius of the die during forming (Figure 11b) and is distributed arbitrarily. Since the flange surface has a constant distance of 1.5 mm to the tool surface, there is no wear in the form of scratches on the surface.

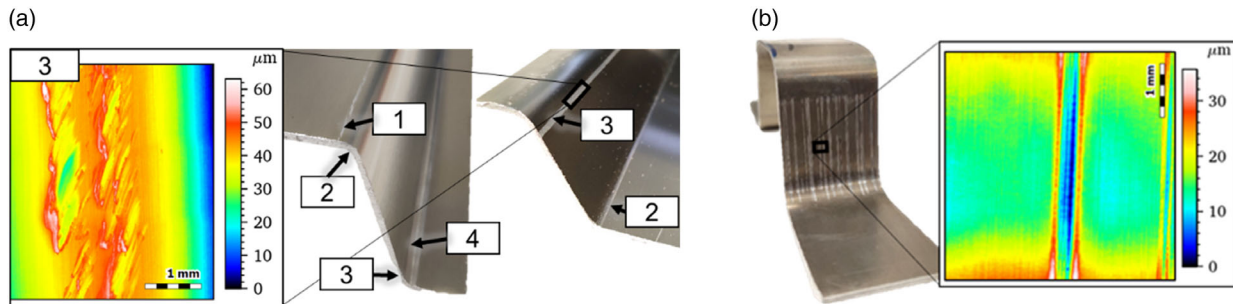


Figure 11. a) Surface quality measurement of the roll formed part and b) the stamped part for the example of the O-process route.

Table 3. R_z and $R_{z(max)}$ values of the scratched area of the formed parts.

Process	Roll forming			Stamping	
	W-Temper	O	T6	W-Temper	O
R_z	2.02	6.23	1.44	2.48	2.56
$R_{z(max)}$	4.69	11.70	4.30	12.7	17.7

For comparison and quantification of the results, the 2D surface profile of the surface of the part is examined for both processes in all cold forming process routes. The evaluation area for roll forming is in location 3 and for stamping at the scratched wall surface. Table 3 shows the comparison of the R_z and $R_{z(max)}$ values. Both forming processes have in common, that the surface quality is better for the higher strength conditions of the material during forming. Stamping in the T6-state shows the least severe scratches, followed by the W-Temper-process routes. While R_z is high for roll forming, $R_{z(max)}$ is high for stamping due to the depth of the scratches. Even the use of oil-based lubricant for the stamping process does not prevent the cause of deep scratches during stamping, especially for the W-Temper- and O-process routes. It should be noted that the different geometries of the roll formed and stamped parts result in different wear conditions. The higher bending angle of the stamped part leads to a higher contact pressure in the tool radius during forming, which results in higher wear. Furthermore, the surface quality can be improved by adjusting the tribological system (e.g., tool surface, tool material, and lubrication) within both processes. Therefore, a general statement on the surface quality within the different forming processes should be taken with caution.

4.1.5. Material Properties after Different Process Routes

Applying different thermomechanical processes on the material by heat treatments and forming influences the material properties. Since the influence on forming history is small, compared to the history of heat treatments, it is neglected within this study. There is a fundamental difference between roll forming and stamping for the W-Temper-process route. For roll forming, SA is conducted inline. Figure 12a shows the preparation of specimens for evaluation of the inline heat treatment during roll forming. As shown in Figure 12b, the yield strength and tensile strength of the inline solution annealed material are slightly

below the initial values for the T6-state, as the inline heat treatment is not performed under perfect conditions. These include the transfer time from the inductor to the quenching chamber, the imperfect temperature profile during induction heating, and the chaotic quenching process in the quenching chamber. A detailed analysis of the heat treatment is published in ref. [13].

For the discontinuous heat treatments, experiments are conducted in order to apply the temperature curves from the temperature-supported process routes to the material. Therefore, the W-Temper experiments are conducted in a contact-heating device according to another study^[23] and the experiments for the O-process route are conducted in the Nabertherm NA 15/65 furnace. Figure 13 shows the influence of the heat treatments on the mechanical properties, dependent on the SA time. For the W-Temper-process route, short SA times lead to improved mechanical properties compared to the as-received T6 material. This underlines the potential of well-designed inline heat treatment.

The results for the O-process route show a high dependency on the SA time. Based on the results, SA time of 10 min seems to be preferable, as the tensile strength, yield strength, and elongation at fracture show the highest values.

Additionally, the HF process routes for stamping are investigated in terms of mechanical properties. Therefore, subsized specimens are cut out of the top surface from the hat profile (Figure 14a) after forming and artificial aging. No forming occurs on the top surface, which means that only the effects of the heat treatment are investigated. Figure 14b shows the results for the stamped hat profile, formed by the divided tool (cold/hot section). For both cooling strategies, the strength is below the as-delivered AA7075 alloy in the T6-state. This might be due to the long transfer time of $t = 15$ s after SA ($t = 15$ min) to the stamping tool, resulting in an unintended temperature drop of the sheet before quenching.

4.1.6. Tailored Properties

Tailored properties can be achieved by targeted quenching during or after the forming processes of roll forming and stamping. This study investigated two different methods for applying tailored properties on the formed part: combined water quenching/air-cooling and HF quenching with separated (hot/cold) tools. The first method applies for both forming processes and the second for stamping. Combined water quenching/air-cooling can be integrated inline into the roll forming process

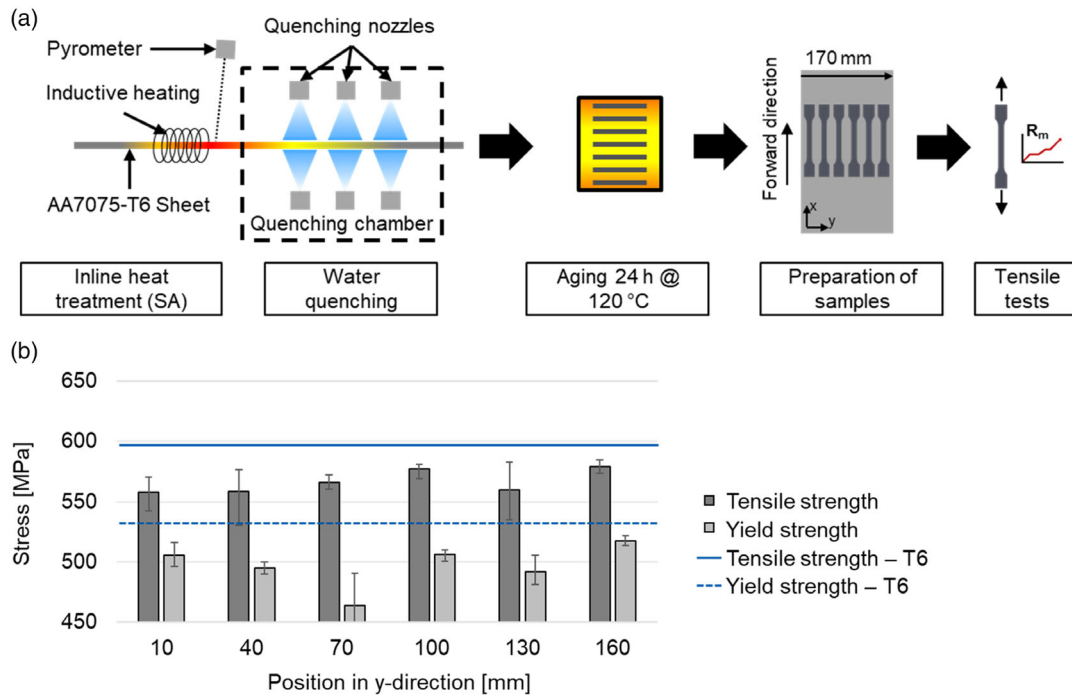


Figure 12. a) Preparation of specimens for evaluating the inline heat treatment during roll forming and b) mechanical properties of the heat-treated material.

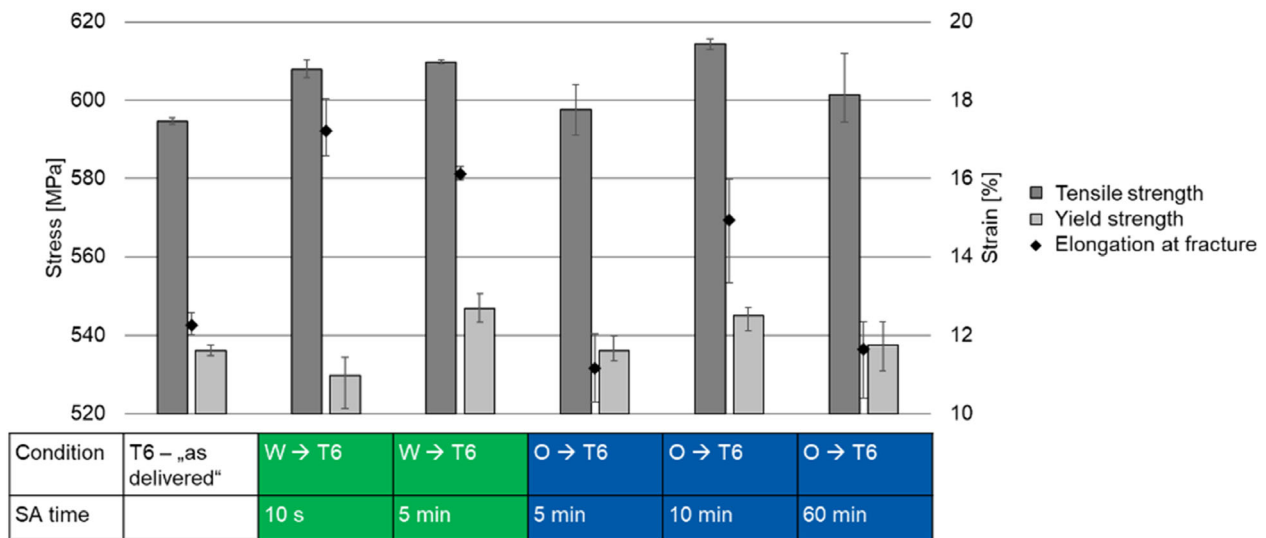


Figure 13. Mechanical properties of the AA7075 alloy after different process routes.

chain and is conducted by targeted quenching after forming. In this study, the experimental setup is simplified to obtain ideal conditions for the quenching process and reproduce the quenching conditions in the quenching chamber. Therefore, samples with a length of 170 mm and a width of 12.5 mm are solution annealed for 5 min at $T = 480\text{ °C}$ in the Nabertherm NA 15/65 furnace. Afterward the samples are partially quenched after a short transfer time of $t = 3\text{ s}$, by holding them in a bucket of water for a defined time (Figure 15a). The sharpness of the

gradient in the transition zone is of great interest, since it is decisive for the properties of the final part. After quenching, artificial aging is performed, followed by hardness measurement. The results for the hardness measurement in the transition zone are shown in Figure 15b. Zhang et al.^[24] underlined the general relationship between the hardness and strength of metals. The influence of different quenching rates on the mechanical properties of the AA7075 alloy is discussed in ref. [5]. To achieve high strength, the quenching rate must be high enough.

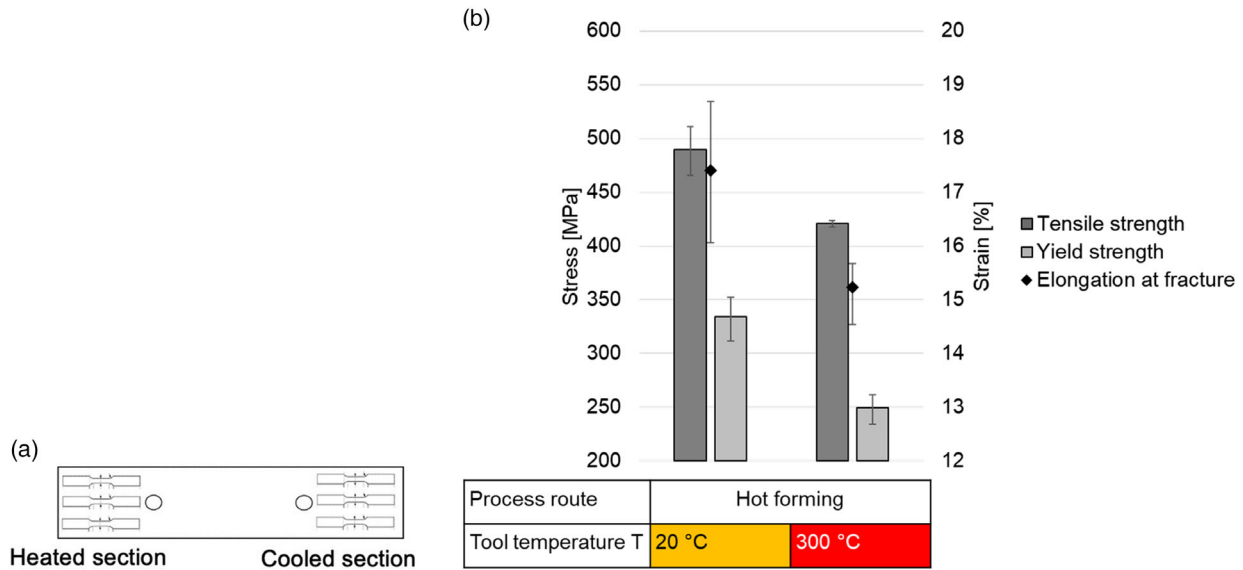


Figure 14. Mechanical properties of the AA7075 alloy after HF and quenching, followed by artificial aging.

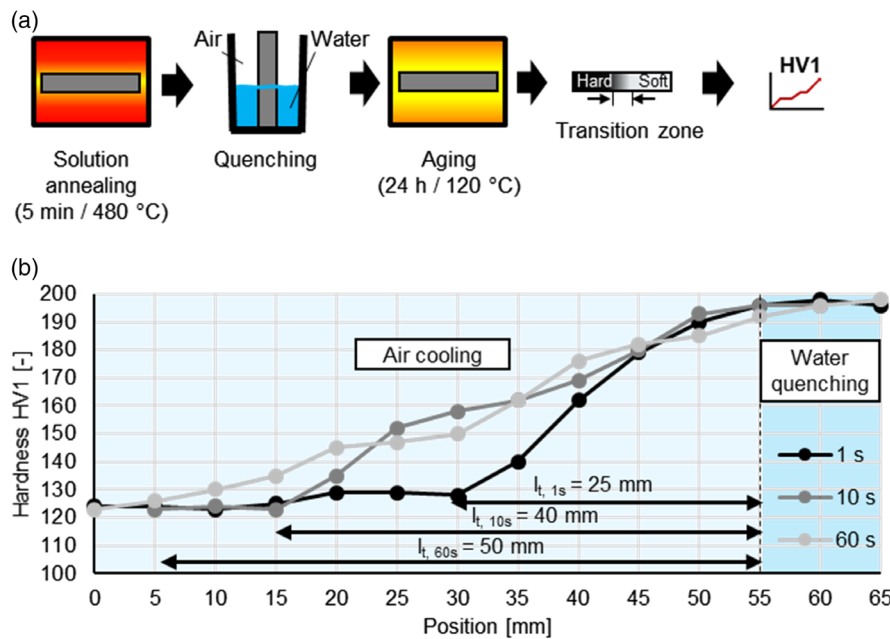


Figure 15. a) Experimental setup for applying tailored properties by combined water quenching/air cooling. b) Hardness measurement for evaluation of the gradient in the transition zone.

The results for targeted quenching show that a short quenching time is advantageous for achieving a small transition zone. For the 1 s quenched specimen, the transition zone is from 30 to 55 mm. Hence, the length of the transition zone is $l_t = 25$ mm from the minimum hardness by air cooling to the maximum hardness by water quenching. The transition zone has a length of $l_t = 40$ mm for the 10 s specimen and a length of $l_t = 50$ mm for the 60 s specimen. Heat transfer leads to self-quenching of the air-cooled material near the water surface. This leads to a larger size of the transition zone for the long quenching times.

The results from the test must be transferred to the actual application with caution, as the quenching conditions in the model test are not identical to the quenching conditions in the quenching chamber.

The experimental setup in Figure 16a is used for stamping to achieve tailored properties in the material. The tailored properties are adjusted during forming and quenching in the separated cold/hot tool. Figure 16b shows the hardness distribution of the hat-shaped profile after the HF-quenching process. The section of the formed part, which was quenched in the heated section of

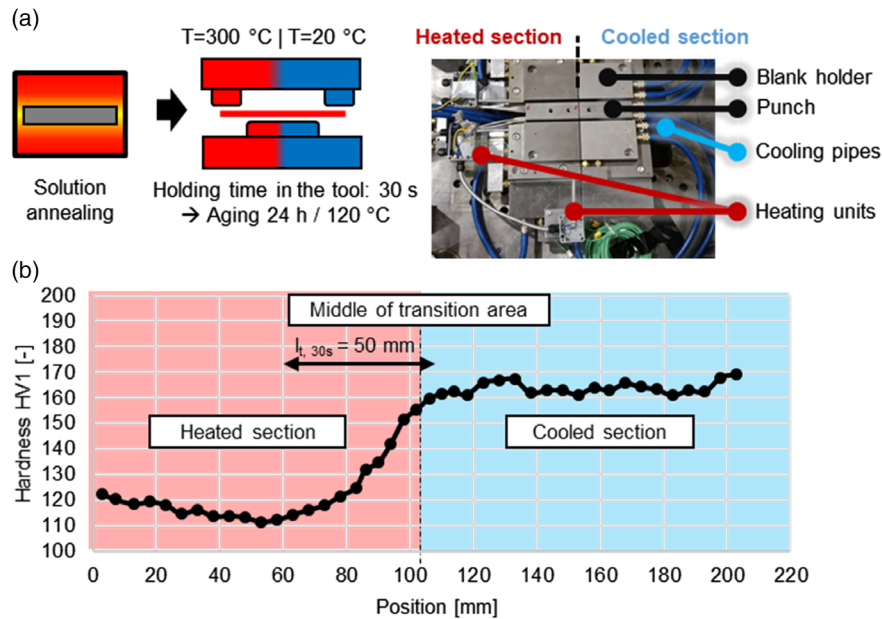


Figure 16. a) Experimental setup for applying tailored properties by HF and targeted quenching. b) Hardness measurement for evaluation of the gradient in the transition zone.

the tool, has comparatively lower hardness values due to the lower cooling rate.

However, in the cold section of the tool, higher hardness is observed in the formed part because of rapid quenching. The transition area has a length of $l_t = 50\text{ mm}$ for the holding time of 30 s in the tool. The influence of different quenching rates on the mechanical properties of the hot formed parts is shown in Section 4.1.5.

Comparing both processes for obtaining tailored properties reveals that the perfect conditions during the combined water quenching and air cooling lead to a small transition zone. Furthermore, the hardness values of air cooling and quenching in the hot part of the tool during HF lead to comparable low hardness values. In contrast, water quenching leads to hardness values of around 200 HV1, while quenching in the cold part of the tool during HF leads to lower hardness values of about 165 HV1. Similar to the strength values, the difference between the two values might be due to the long transfer time after SA to the stamping tool.

4.2. Ecological and Economic Analysis of the Process Chains

4.2.1. Production Rate

The bottlenecks within the various process routes are identified to estimate the production rate. The T6 process has the highest production rate, since there is no time-consuming heat treatment in the process chain. Each heat treatment during the process lowers the production rate, since heat treatment time is much longer than forming or transfer processes during the process routes. One exception is the W-Temper process route for roll forming, where the preheat treatment is feasible inline. This is an advantage for the production rate of this process route. However, artificial aging is discontinuous after forming and lowers the production rate. The W-Temper- and HF process routes for stamping have a slightly

lower production rate, since the preheat treatment is discontinuous here. Artificial aging (24 h) and soft annealing (10 h) are the most time-consuming heat treatments. Thus, the O-process routes for both forming processes have the lowest production rates.

4.2.2. Energy Efficiency

The most energy-consuming parts of the process chains are the heat treatments, especially the long-term treatments. Forming energy is small, compared to the energy and energy dissipation for the heat treatments. Therefore, this energy is neglected in the analysis. Besides the T6-process route, all process routes require at least two heat treatments. The first is to achieve a higher formability of the material and the second is to increase the material's performance. Soft annealing is the most energy consuming due to the least advantageous combination of high temperature, holding time, and defined temperature cycles. Although the time for artificial aging is higher, the temperature is significantly lower.

For the W-Temper-process routes, there is a difference between the forming processes regarding the heating mechanism for the preheat treatment. During roll forming, heat treatment is conducted inline by induction heating. Preheat treatment for stamping involves SA in a furnace for 15 min. Energy losses are highly dependent on the heating system. However, a precise determination of energy efficiency is not possible. For increasing energy efficiency, heat recovery is an option for returning the lost heat in the form of quenching heat or waste heat from the furnaces to the heating process.

5. Conclusion

The summary of the forming processes and process routes, including process design, product quality evaluation, productivity,

Forming process	Process route	Process design			Product quality				Productivity	Energy efficiency
		Effort	Requirements for FE-model	Requirements for machine and tools	Formability	Geometrical accuracy	Mechanical properties	Surface quality		
Roll forming	T6	+	+	++	--	-- (expected)	++ (expected)	++ (expected)	++	++
	W	--	+	+	++	++	+	+	+	+
	O	+	+	+	++	++	++	-	-	--
Stamping	T6	+	++	-	-	--	++	+	+	++
	W	+	++	-	++	-	++	-	-	+
	O	+	++	-	++	-	++	--	-	--
	Hot forming	--	-	-	++	+	-	--	-	-

Figure 17. Evaluation matrix for forming processes and process routes.

and energy efficiency, is shown in **Figure 17**. A recommendation of an appropriate process route, depending on individual requirements, is provided. The process routes for applying tailored properties on the formed parts are not considered in the evaluation.

The T6-process routes offer a high potential, since process design is simple, and product quality, productivity, and energy efficiency are high. Disadvantages are the low formability of the AA7075 alloy in the T6-state and the high springback after forming. This implies the need to prioritize the individual assessment parameters for the evaluation of product quality. Advantages such as the good mechanical properties and surface quality of the T6 process route are invalid if a component cannot be produced due to poor formability.

Temperature-supported process routes are helpful to increase formability and reduce springback significantly, which allow the manufacturing of more complex profiles. However, the main disadvantage for the product quality is the surface quality of the part, which can be improved by optimizing the process parameters related to the tribological system. Further disadvantages are the lower productivity and energy efficiency and thus higher costs. Additionally, the W-Temper-process route for roll forming and the HF process route for stamping require an accurate process design with low unintended temperature differences of the material during the heat treatments. As shown in the experiments, slight temperature differences lead to significant differences in the material properties. Unintentional temperature differences are caused for example by the sheet transfer after SA, inhomogeneous heating and quenching conditions, and the choice of wrong parameters (e.g., SA time). Therefore, the authors recommend the precise evaluation of the process route with regard to temperature control as well as the performance of preliminary tests that accurately simulate the temperature–time curves of the entire process chain. Thus, it can be verified that the final components preserve the specified mechanical properties.

Further potential for forming the AA7075 alloy is offered by applying tailored properties on the produced profiles. Again, a detailed process design in terms of temperature control is necessary to achieve a small transition area and good mechanical properties. Two methods are investigated to apply tailored

properties: combined water quenching/air-cooling and HF quenching with separated (hot/cold) tools. The minimum size of the transition area ($l_t = 25$ mm) within this investigation was obtained by combined water quenching/air cooling with a short quenching time. HF and quenching with separated tools lead to a size of the transition zone of $l_t = 50$ mm, which still is a sharp gradient for long profiles.

Acknowledgements

The authors gratefully acknowledge financial support from the Hessen State Ministry for Higher Education, Research and the Arts- Initiative for the Development of Scientific and Economic Excellence (LOEWE) for the Project ALLEGRO (Subprojects A1 and A2).

Open Access funding enabled and organized by Projekt DEAL.

Conflict of Interest

The authors declare no conflict of interest.

Data Availability Statement

Research data are not shared.

Keywords

7075, aluminum, hat profiles, roll forming, stamping, tailored properties

Received: December 23, 2022

Revised: February 23, 2023

Published online: March 22, 2023

[1] K. Zheng, Y. Dong, J.-H. Zheng, A. Foster, J. Lin, H. Dong, T. A. Dean, *Mater. Sci. Eng., A* **2019**, 761, 138017.

[2] N. Sotirov, P. Simon, C. Chimani, D. Uffelmann, C. Melzer, *KEM* **2012**, 504–506, 955.

- [3] E. Sáenz de Argandoña, L. Galdos, R. Ortubay, J. Mendiguren, X. Agirretxe, *Key Eng. Mater.* **2015**, 651–653, 199.
- [4] B.-A. Behrens, L. Lippold, J. Knigge, *Prod. Eng.* **2013**, 7, 319.
- [5] S. V. Sajadifar, T. Suckow, B. Heider, M. Oechsner, P. Groche, T. Niendorf, *Materialwiss. Werkstofftech.* **2022**, 53, 1479.
- [6] E. Scharifi, R. Knoth, U. Weidig, *Procedia Manuf.* **2019**, 29, 481.
- [7] J. Mendiguren, E. S. de Argandona, L. Galdos, *IOP Conf. Ser.: Mater. Sci. Eng.* **2016**, 159, 12026.
- [8] H. Wang, Y.-B. Luo, P. Friedman, M.-H. Chen, L. Gao, *Trans. Nonferrous Met. Soc. China* **2012**, 22, 1.
- [9] Deutsches Institut für Normung – DIN, *Wärmebehandlung von Aluminium-Knetlegierungen*, Beuth Verlag GmbH, Berlin **1989**
- [10] T. Suckow, J. Schroeder, P. Groche, *Prod. Eng.* **2021**, 15, 573.
- [11] S.-K. Lee, J.-S. Lee, J.-H. Song, J.-Y. Park, S. Choi, W. Noh, G.-H. Kim, *Procedia Manuf.* **2018**, 15, 751.
- [12] G. Halmos, *Roll Forming Handbook*, Taylor & Francis Group, Boca Raton, FL **2006**.
- [13] T. Suckow, P. Groche, *KEM* **2022**, 926, 690.
- [14] R. Brandegger, *User Manual: Ubeco PROFIL Roll Form Design Software: PROFIL Release 6.2*, UBECO GmbH, Iserlohn, Germany **2022**.
- [15] data M Sheet Metal Solutions GmbH, *COPRA RF Sections*, data M Sheet Metal Solutions GmbH, Valley, Germany **2023**.
- [16] A. E. Tekkaya, *J. Mater. Process. Technol.* **2000**, 103, 14.
- [17] P. Groche, C. Mueller, T. Traub, K. Butterweck, *Steel Res. Int.* **2014**, 85, 112.
- [18] Deutsches Institut für Normung – DIN, *Prüfung metallischer Werkstoffe - Zugproben*, Beuth Verlag GmbH, Berlin **2009**.
- [19] K. Kumar, A. Pooleery, K. Madhusoodanan, R. N. Singh, J. K. Chakravarty, B. K. Dutta, R. K. Sinha, *Procedia Eng.* **2014**, 86, 899.
- [20] Deutsches Institut für Normung – DIN, *Kaltprofile aus Stahl: Technische Lieferbedingungen*, Beuth Verlag GmbH, Berlin **2003**.
- [21] A. S. Galakhar, J. D. Gates, W. J. T. Daniel, P. A. Meehan, *Wear* **2011**, 271, 2728.
- [22] Ö. N. Cora, A. Ağcayazı, K. Namiki, H. Sofuoğlu, M. Koç, *Tribol. Int.* **2012**, 52, 50.
- [23] L. Schell, P. Groche, *DDF* **2022**, 414, 95.
- [24] P. Zhang, S. X. Li, Z. F. Zhang, *Mater. Sci. Eng., A* **2011**, 529, 62.